

# Preparation of Poly(4'-oxy-4-biphenylcarbonyl) Needlelike Crystals with the Aid of Copolymerization

Naomi Yoshida,<sup>†</sup> Yasuhiro Kurihara,<sup>†</sup> Shin-ichiro Kohama,<sup>†</sup> Tetsuya Uchida,<sup>‡</sup> Shinichi Yamazaki,<sup>†</sup> and Kunio Kimura<sup>\*,†</sup>

Graduate School of Environmental Science, Okayama University, 3-1-1Tsushima-naka, Okayama 700-8530 Japan, and Graduate School of Natural Science and Technology, Okayama University, 3-1-1Tsushima-naka, Okayama 700-8530 Japan

Received January 6, 2008; Revised Manuscript Received August 28, 2008

**ABSTRACT:** Preparation of poly(4'-oxy-4-biphenylcarbonyl) (POBP) needlelike crystals was examined by using reaction-induced crystallization of oligomers during copolymerization of 4-(4-acetoxyphenyl)benzoic acid (APBA) and 4-acetoxybenzoic acid (ABA). Polymerizations were carried out in aromatic solvent at various ABA molar ratios in feed ( $\chi_f$ ). When the  $\chi_f$  was 20–10 mol %, starlike aggregates of needlelike crystals and fibrillated slablike crystals were separately formed, exhibiting similar morphology to poly(4-oxybenzoyl) and POPB crystals. 4-(Oxyphenyl)benzoyl (OPB) homo-oligomers and co-oligomers rich in OPB moiety were more rapidly precipitated due to the lower solubility, and the slablike crystals were formed. Afterward, 4-oxybenzoyl (OB) homo-oligomers and the co-oligomers rich in OB moiety were precipitated to form spindlelike crystals. The OPB homo-oligomers and the co-oligomers rich in OPB moiety were continuously crystallized on both crystals due to the high degree of supersaturation, and the spindlelike crystals grew to the needlelike crystals mainly comprised of POBP. Copolymerization of 4-(4-acetoxybenzoyloxy)benzoic acid and APBA at  $\chi_f$  of 10 mol % yielded the needlelike crystals without coexisting fibrillated slablike crystals. This result provides a new methodology for morphology control with the aid of copolymerization.

## Introduction

Morphology is of great importance to control the properties of polymer materials.<sup>1</sup> Especially, rigid-rod aromatic polyesters such as poly(4-oxybenzoyl) (POB) and poly(4'-oxy-4-biphenylcarbonyl) (POBP) have been expected to possess many excellent properties such as mechanical properties including strength and modulus, thermal stability, chemical resistance and so on, and they have received great attention as high performance materials.<sup>2–6</sup> However, these polyesters do not exhibit meltability and solubility, and the intractability makes them difficult to process by conventional processing procedures. Morphology control of these aromatic polyesters has been studied by using reaction-induced phase separation of oligomers and POB whiskers were prepared by the polymerization of 4-acetoxybenzoic acid (ABA) in poor solvents at 330 °C.<sup>7–11</sup> These POB whiskers were formed via the crystallization of oligomers and the subsequent solid-state polymerization in or on the precipitated needlelike oligomer crystals. The molecular chains are aligned along the long axes of the whiskers. POBP whiskers were not obtained under the same conditions as those of the POB whiskers and only fibrillated slablike crystals were formed.<sup>12</sup> The POPB whiskers were prepared only by the extremely high temperature polymerization of 4-(4-acetoxyphenyl)benzoic acid (APBA) at 400 °C.<sup>13</sup> APBA had also been polymerized from the bulk melt, and when polymerized at 270 °C, large blocks of fibrous material were formed.<sup>14</sup>

It has been well-known that copolymerization usually lowers the crystallizability and the clear morphology of the homopolymer crystals was drastically damaged. Although some copolyester crystals have been successively prepared by constrained thin film polymerization,<sup>15–17</sup> it is generally difficult to control the morphology of the crystals in copolymerization systems.

However, if the oligomers having particular composition can be selectively precipitated based on the difference of solubility, a clear morphology of the crystals can be created even in a copolymerization and terpolymerization system by using the crystallization of oligomers.<sup>18–24</sup>

This paper describes new findings on the fabrication of the POBP needlelike crystals with the aid of copolymerization of APBA and ABA.

## Experimental Section

**Materials.** ABA was purchased from TCI Co. Ltd. and purified by recrystallization from ethyl acetate. APBA was synthesized according to previous papers.<sup>12–14</sup> A mixture of isomers of dibenzyltoluene (DBT) was purchased from Matsumura Oil Co. Ltd. (Barrel Therm 400; MW = 380 and bp = 382 °C) and purified by distillation under reduced pressure (160–170 °C/0.3 mmHg). 4-(4-Acetoxybenzoyloxy)benzoic acid (ABAD) was synthesized as an ABA dimer according to a previous procedure.<sup>25</sup>

**Measurements.** Morphology of the products was observed on a HITACHI S-3500N scanning electron microscope (SEM) at 20 kV and a JEOL 2000EX II transmission electron microscope (TEM) at 200 kV. Selected-area electron diffraction patterns were also taken on the same transmission electron microscope. Samples for SEM observation were dried in air at room temperature and sputtered with platinum–palladium. Samples for TEM observation were prepared by depositing the precipitate suspension in acetone onto carbon grid and dried in air at room temperature. Samples for evaluation of the thickness were shadowed with platinum–palladium. Average shape parameters of the products were determined by taking the average of over 150 observation values. Chemical structure of the polymers was measured on a JASCO FT-IR-410 Itron IRT30 microscopic FT-IR spectrometer. Aperture size was 20–40  $\mu\text{m}$ . A powder pattern of wide-angle X-ray scattering (WAXS) was recorded on a RIGAKU MiniFlex diffractometer with nickel-filtered Cu K $\alpha$  radiation at 30 kV and 15 mA with a scanning rate of 1 deg $\cdot$ min<sup>-1</sup>. Composition of copolymers was determined on a <sup>1</sup>H NMR JEOL AL300 SC-NMR spectrometer operating at 300 MHz after their hydrolysis. DMSO-d<sub>6</sub> was used as a solvent. The molar ratio of 4-oxybenzoyl (OB) moiety in the precipitated

\* To whom correspondence should be addressed. Telephone and Fax: +81-86-251-8902. E-mail: polykim@cc.okayama-u.ac.jp.

<sup>†</sup> Graduate School of Environmental Science, Okayama University.

<sup>‡</sup> Graduate School of Natural Science and Technology, Okayama University.

Table 1. Results of Copolymerization of ABA with APBA<sup>a</sup>

run no.	raw materials <sup>b</sup>	$\chi_f^c$ (mol %)	yield (%)	$\chi_p^d$ (mol %)	morphology
1	ABA + APBA	100	59	100	needle
2	ABA + APBA	99	53	>99	fibril
3	ABA + APBA	95	58	96	fibril
4	ABA + APBA	90	47	92	sphere
5	ABA + APBA	50	48	51	sphere
6	ABA + APBA	25	49	23	sphere
7	ABA + APBA	20	52	15	fibrillated slab, needle
8	ABA + APBA	10	64	6	fibrillated slab, needle
9	ABA + APBA	0	52	0	slab
10	ABAD + APBA	25	68	20	sphere
11	ABAD + APBA	20	69	13	needle
12	ABAD + APBA	10	64	8	needle

<sup>a</sup> Polymerizations were carried out in DBT at 330 °C and a concentration of 1.0% for 6 h. <sup>b</sup> ABAD stands for the dimer of ABA. <sup>c</sup> Molar ratio of OB moiety in feed. <sup>d</sup> Molar ratio of OB moiety in precipitates.

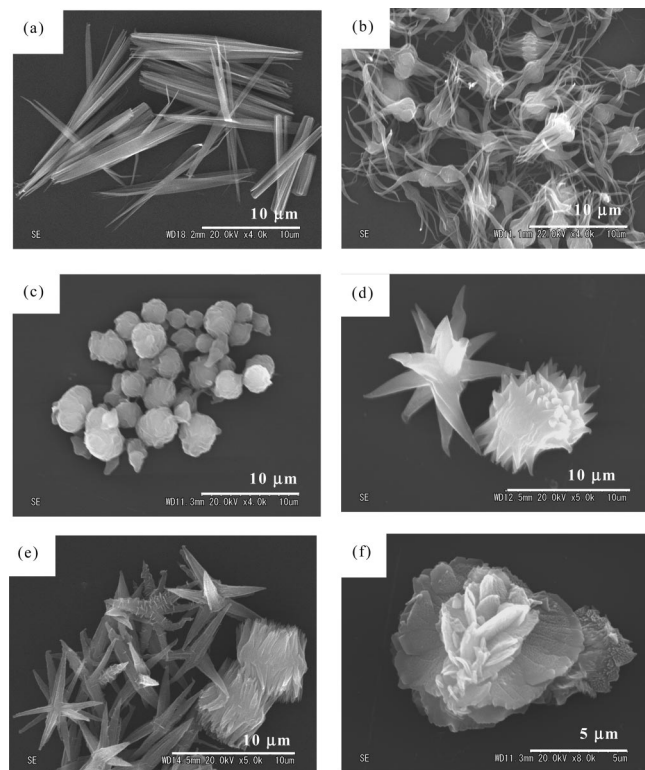


**Figure 1.** Morphologies of precipitates prepared from ABA and APBA at 330 °C and  $\chi_f$  of (a) 100 mol % (run no. 1), (b) 96 mol % (run no. 3), (c) 90 mol % (run no. 4), (d) 20 mol % (run no. 7), (e) 10 mol % (run no. 8), and (f) 0 mol % (run no. 9).

crystals ( $\chi_p$ ) were calculated by using the peak of aromatic proton of 4-hydroxybenzoic acid (2H, d,  $\delta$  = 7.78 ppm) and that of 4-(4-hydroxyphenyl)benzoic acid (2H, d,  $\delta$  = 7.96 ppm) as follows:

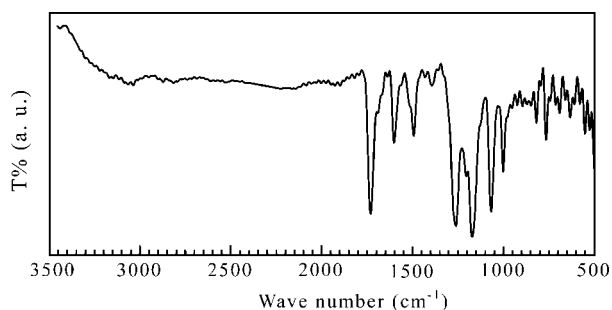


**Figure 2.** IR spectra of precipitates prepared at  $\chi_f$  of 10 mol % (run no. 8).

$$\chi_p(\text{mol \%}) = \frac{[\text{OB}]}{[\text{OB}] + [\text{OPB}]} \times 100$$

where OB and OPB stand for 4-oxybenzoyl moiety and 4-(4-oxyphenyl)benzoyl moiety, respectively.

Matrix-assisted laser desorption/ionization time-of-flight (MALDI-TOF) mass spectrometry was performed on a Bruker Daltonics AutoFLEX MALDI-TOF MS system operating with a 337 nm N<sub>2</sub> laser. Spectra were obtained in the linear positive mode with accelerating potential of 20 kV. Mass was calibrated with angiotensin I (MW 1296.69) and insulin B (MW 3496.96) of a Sequazyme peptide mass standard kit. Samples were prepared by the evaporation-grinding method, and then measured in dithranol as a matrix doped with potassium trifluoroacetate salt and sodium trifluoroacetate salt according to the reported procedure.<sup>26–28</sup>

**Polymerization.** Polymerization at molar ratio of ABA in feed ( $\chi_f$ ) of 10 mol % is described as a typical example. ABA (0.019 g, 0.106 mmol), APBA (0.245 g, 0.957 mmol) and 20 mL of DBT

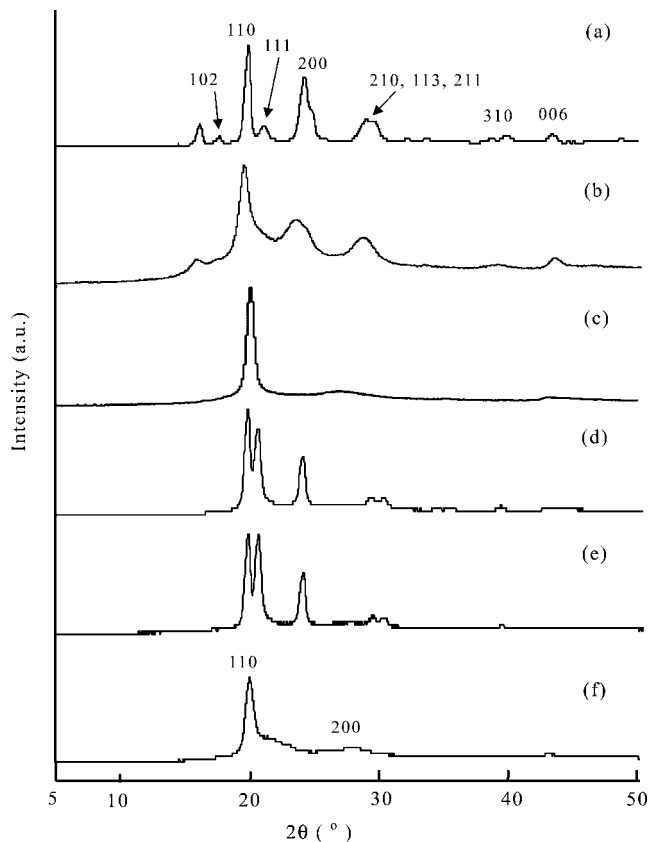


**Figure 3.** WAXS intensity profiles of precipitates prepared at  $\chi_f$  of (a) 100 mol % ABA (run no. 1), (b) 90 mol % ABA (run no. 4), (c) 25 mol % ABA (run no. 6), (d) 10 mol % ABA (run no. 8), (e) 10 mol % ABA (run no. 8), (f) 0 mol % ABA (run no. 12).

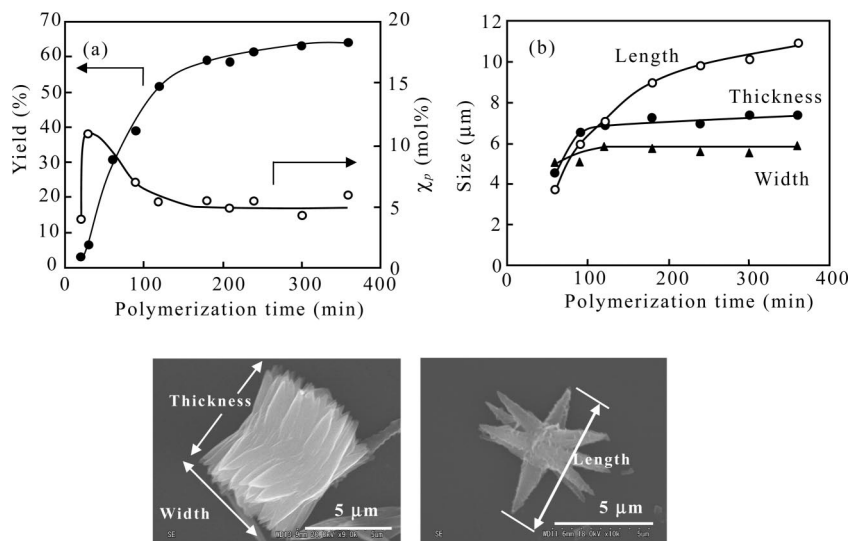


**Figure 4.** Plots of (a) yield and  $\chi_p$ , and (b) size parameters of the precipitated crystals as a function of time in copolymerization of ABA and APBA at  $\chi_f$  of 10 mol %.

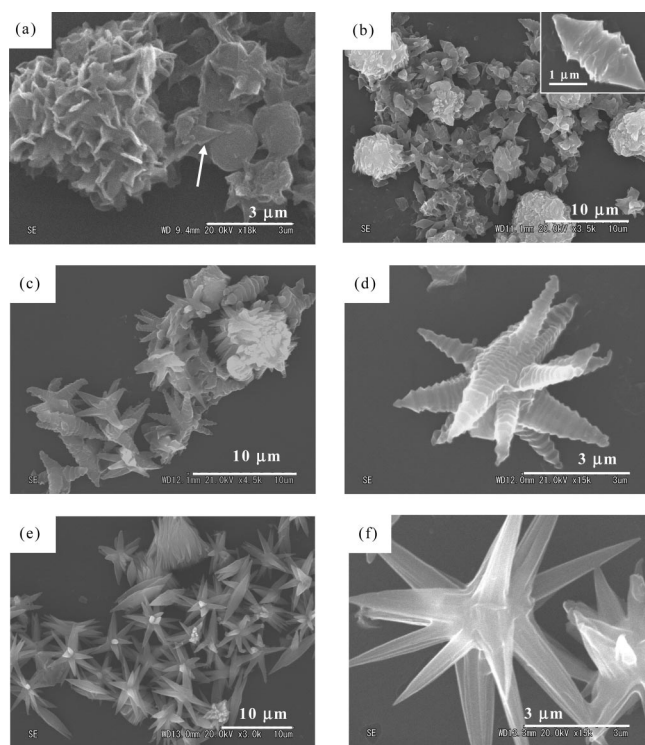


**Figure 5.** Morphology of the precipitated crystals prepared from ABA and APBA at  $\chi_f$  of 10 mol % for (a) 0.5 h, (b) 1 h, (c), (d) 1.5 h, and (e) 3 h. Precipitates prepared for 1.5 h after washing with KOH solution are shown in (f).

were placed in a cylindrical flask equipped with a mechanical stirrer and a gas inlet tube. Polymerization concentration, defined as (calculated polymer weight 0.2 g/solvent volume 20 mL)  $\times$  100 in this study, was 1.0%. The reaction mixture was heated under a slow stream of nitrogen up to 330 °C with stirring. Stirring was stopped when the monomers were entirely dissolved. Temperature was maintained at 330 °C for 6 h. The precipitates were collected by vacuum filtration at 330 °C, and washed with *n*-hexane and then acetone. The filtrate was poured into *n*-hexane and the precipitated oligomers, which were dissolved at 330 °C in DBT, were recovered by filtration. Other compositions were prepared in a similar manner.

**Kinetic Study.** ABA (0.30 g, 1.67 mmol) or APBA (0.26 g, 1.02 mmol) and 20 mL of DBT were placed into a 40 mL cylindrical vessel equipped with gas inlet and outlet tubes. Initial concentrations

of ABA and APBA were  $8.3 \times 10^{-2}$  and  $5.1 \times 10^{-2}$  mol·L<sup>-1</sup>, respectively. The mixture was placed into an oil bath and heated up to polymerization temperature under a slow stream of nitrogen with stirring. Polymerization was monitored by the measurement of the evolved acetic acid trapped in the water at different times. The amount of acetic acid produced at a given time was determined by titration with 0.1 mol·L<sup>-1</sup> sodium hydroxide solution.

## Results and Discussion

**Copolymerization of ABA and APBA.** Polymerizations were carried out at various molar ratios of ABA in feed ( $\chi_f$ ) at a concentration of 1.0%, which was defined as percentage based on polymer weight and solvent volume. Polymerization temperature was 330 °C. Results are presented in Table 1 and morphologies of precipitates are shown in Figure 1. Needlelike POB crystals were formed by the polymerization of ABA ( $\chi_f$  of 100 mol %) in DBT. The average length and width were 10.9 and 1.5  $\mu\text{m}$ , respectively. On the other hand, aggregates of slablike POBP crystals were obtained by the polymerization of APBA ( $\chi_f$  of 0 mol %). The average thickness of the slablike crystals was 0.1  $\mu\text{m}$ . The morphology of the precipitates was drastically changed by the copolymerization of these two monomers. Fibrillar crystals having spherical parts in the center were formed at  $\chi_f$  of 95 mol %. The clear crystal habit was extinguished and spherical precipitates were obtained at  $\chi_f$  of 90–25 mol %. This drastic change in the morphology is mainly attributed to the following reasons; the copolymerization lowers the crystallizability of oligomers and the co-oligomers are liable to be precipitated by liquid–liquid phase separation because of the reduction of the freezing point.<sup>13,14</sup> When the value of  $\chi_f$  was 20–10 mol %, two different types of crystals were independently formed, these were starlike aggregates of needlelike crystals and fibrillated slablike crystals. Although the slablike crystals were fibrillated, these morphologies are roughly similar to those of the POB and POBP crystals. The values of  $\chi_p$  of the mixtures of precipitates prepared at  $\chi_f$  of 20 and 10 mol % determined by NMR were 15 and 6 mol %, respectively. These precipitates were totally insoluble in organic solvents because of high molecular weight, and their chemical structure was confirmed by IR spectroscopy. The IR spectrum of the precipitates prepared at  $\chi_f$  of 10 mol % is shown in Figure 2. The peak for C=O of the ester group appeared at 1731 cm<sup>-1</sup>, and the characteristic peaks of monomers completely disappeared, such as acetyl groups and carboxyl groups. This spectrum indicates the formation of high molecular weight



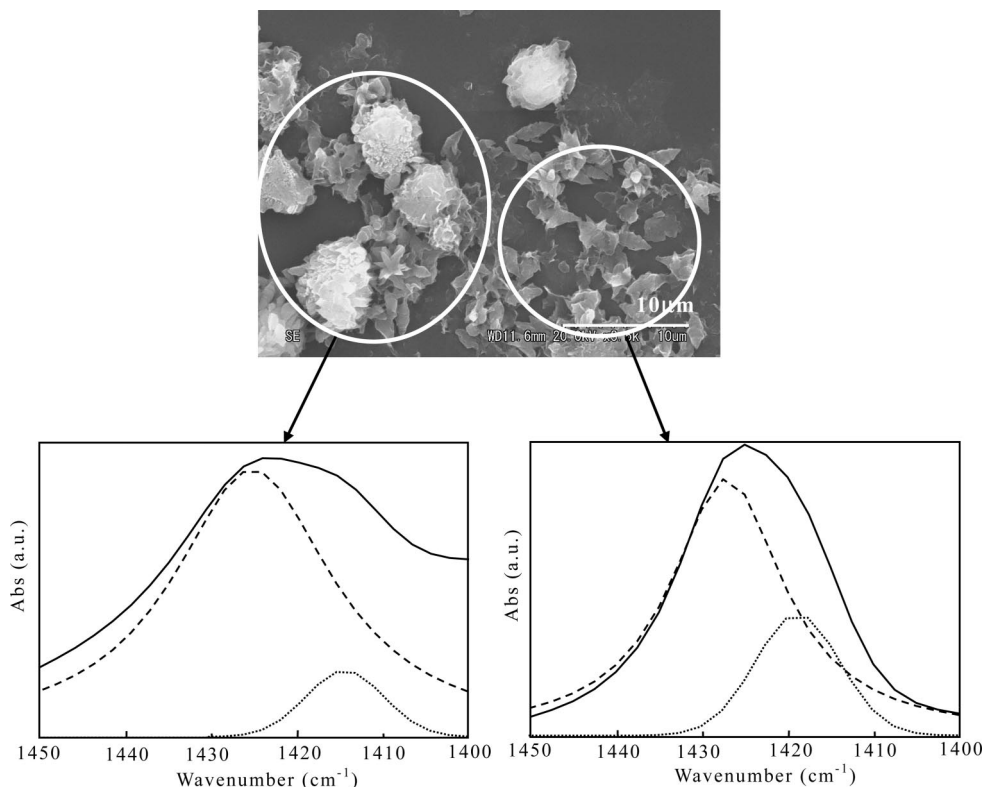


**Figure 6.** Microscopic IR spectra of precipitates prepared from ABA and APBA at  $\chi_f$  of 10 mol % for 1 h.

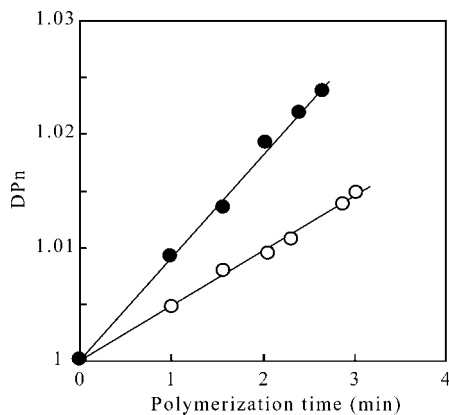


**Figure 7.** Kinetics of second order reaction of (○) ABA and (●) APBA in DBT at 330 °C.

polyesters. WAXS intensity profiles of the precipitates prepared at  $\chi_f$  of 100, 90, 30, 10, and 0 mol % are shown in Figure 3. Diffraction peaks of POB and POBP crystals could be assigned according to the previously reported orthorhombic unit cell of a POB<sup>29</sup> and POBP crystal<sup>12</sup> as indexed in Figure 3. Diffraction peaks became broader even at  $\chi_f$  of 90 mol % and the crystallinity became low. In the profile of the precipitates prepared at  $\chi_f$  of 25 mol %, one strong peak was clearly observed at  $2\theta$  of 20.0° and crystal structure tends to change from orthorhombic to hexagonal structure. However, the profile of the precipitates prepared at  $\chi_f$  of 10 mol % was quite different and six sharp peaks were clearly observed at  $2\theta$  of 19.3, 20.0, 23.5, 28.9, 29.8 and 39.0°. Although the value of  $\chi_p$  was only 6 mol %, five characteristic peaks of the POB crystals at  $2\theta$  of 19.3, 23.5, 28.9, 29.8 and 39.0° were detected clearly besides the peak of the POBP crystals. Thus both POB and POBP crystals existed in these precipitates, which are starlike aggregates of needlelike crystals and fibrillated slablike crystals.

In order to clarify the crystal formation mechanism, yields and the values of  $\chi_p$  of the precipitated crystals were examined in the course of polymerization at  $\chi_f$  of 10 mol %. Further, average length of the needlelike crystals, and average width and thickness of the fibrillated slablike crystals were also measured. These results are plotted in Figure 4. The morphological changes are shown in Figure 5. The yield increased rapidly to 60% from 0.5 to 3 h, and thereafter it increased gradually to 64%. The length of the needlelike crystals prepared for 1 h was 3.8  $\mu\text{m}$  and then it increased to 10.9  $\mu\text{m}$  until 6 h. The width and the thickness of the fibrillated slablike crystals were 5.0 and 4.5  $\mu\text{m}$  after 1 h, respectively. The width increased slightly during the initial stage of polymerization to ca. 6  $\mu\text{m}$  and then remained constant. The thickness increased rapidly to 6.8  $\mu\text{m}$  until 2 h and then it increased slightly to 7.4  $\mu\text{m}$  until 6 h. Oligomers precipitated after 3 h were mainly consumed to increase of the length of the needlelike crystals. In contrast to this, the value of  $\chi_p$  increased rapidly from 20 min to 0.5 h from 4 to 11 mol %. Then it decreased until 2 h and became constant at ca. 6 mol %. This maximum in the value of  $\chi_p$  suggests that first the oligomers rich in OPB moiety were precipitated and then those rich in OB moiety precipitated intensively from 20 min to 2 h with precipitating the oligomers rich in OPB moiety. The crystals prepared for 0.5 h contained both aggregates of slablike crystals and spindlelike crystals having very sharp tips (arrow in Figure 5a). Then each type grew independently with time. The spindlelike crystals grew to the needlelike crystals as shown in Figure 5b. Interestingly the initial needlelike crystals showed lamella-stacking structures. The needlelike crystals prepared for 1.5 h were placed in aqueous KOH solution without stirring at 25 °C to observe the inner structure. As shown in Figure 5f, the lamellae-stacking structure was not observed in the inner structure and streaks along the long axis of the needlelike crystals were seen. After 3 h, the trace of the lamellae-stacking structure was not observed and the surface of the needlelike crystals became very smooth. It had been reported that the POB whiskers were formed by the spiral growth of lamellae and the

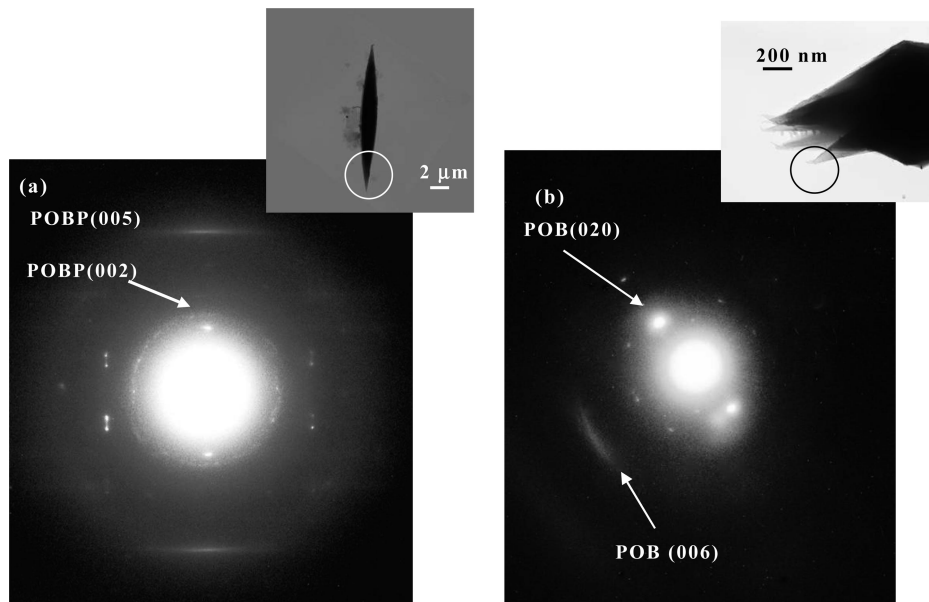


**Figure 8.** Selected area electron diffraction patterns of crystals prepared from ABA and APBA at  $\chi_f$  of 10 mol % for (a) 6 h and (b) 1 h.



**Figure 9.** Shadowed image of a spindlelike crystal prepared from ABA and APBA at  $\chi_f$  of 10 mol % for 1 h.

subsequent polymerization in the them.<sup>7–9</sup> The initial morphology of the POB whiskers are the spindlelike crystals formed by stacking of lamellae. The morphology of the spindlelike crystals formed in the polymerization at  $\chi_f$  of 10 mol % resembles the initial morphology of the POB whiskers. This morphological resemblance suggested that the needlelike crystals are formed by the spiral growth of oligomer lamellae. The chemical structures of the needlelike crystal and the fibrillated slablike crystals prepared for 1 h were analyzed on a microscopic FT-IR spectrometer. The spectra are shown in Figure 6. The measured spectra were resolved in the range of 1450–1400  $\text{cm}^{-1}$  by using the combined function of Lorentzian and Gaussian to detect the aromatic bands corresponding to the 1,4-phenylene and 4,4'-biphenyl moieties at 1415 and 1425  $\text{cm}^{-1}$ ,

respectively. The intensity ratios of these two bands ( $I(1415 \text{ cm}^{-1})/I(1425 \text{ cm}^{-1})$ ) of the spindlelike crystals and the fibrillated slablike crystals were 0.5 and 0.3 respectively. This result indicates that the spindlelike crystals contained more OB moiety.

The difference in the morphology and the composition of these two crystals suggests that they are formed independently because of the difference in the formation rate and the phase separation behaviors of the oligomers on their compositions. The formation rates of the oligomers were estimated by the self-condensation reaction of ABA and APBA in DBT at 330 °C. The self-condensation reactions of these monomers obeyed second order kinetics and the rate constants ( $k_2$ ) were estimated from the plots of number average degree of polymerization (DP<sub>n</sub>) calculated from the evolved acetic acid as a function of polymerization time as shown in Figure 7. The rate constants ( $k_2$ ) of ABA and APBA at 330 °C were estimated as  $9.7 \times 10^{-2}$  and  $12.3 \times 10^{-2} \text{ L} \cdot \text{mol}^{-1} \cdot \text{min}^{-1}$ , respectively. The value of  $k_2$  of APBA is 1.3 times higher, thus APBA polymerizes slightly faster than ABA. The solubility of the homo-oligomers into DBT was estimated by the temperature at which the monomers were entirely dissolved during heating ( $T_s$ ) and the time when the solution became turbid at 330 °C due to the precipitation of oligomers ( $t_t$ ). The values of  $T_s$  of ABA and APBA were 170 and 260 °C respectively, thus APBA is less soluble than ABA. The values of  $t_t$  of ABA and APBA were 11 and 6 min, then the 4-(4-oxyphenyl)benzoyl (OPB) homo-oligomers were more rapidly precipitated than the OB homo-oligomers. These results imply that the oligomers rich in OPB moiety are more rapidly formed and precipitated prior to the precipitation of those rich in OB moiety. These results on the formation rates of ABA and APBA and the solubility of them are consistent with the results in Figure 4.

Selected area electron diffractions of the tip part of the needlelike crystals prepared at  $\chi_f$  of 10 mol % for 6 h and the spindlelike crystals prepared for 1 h were taken to determine the details of the structure. The diffraction patterns are shown in Figure 8. Both diffraction patterns were not fiber pattern with cylindrical symmetry; sharp spots were observed. The reflections obtained from the tip parts of the needlelike crystals prepared for 6 h were assignable as POBP, as shown in Figure 8a; therefore, the tip parts of the needlelike crystals were comprised of POBP crystals. {002} and {005} reflections of POBP were clearly detected on the meridian corresponding to the long axis

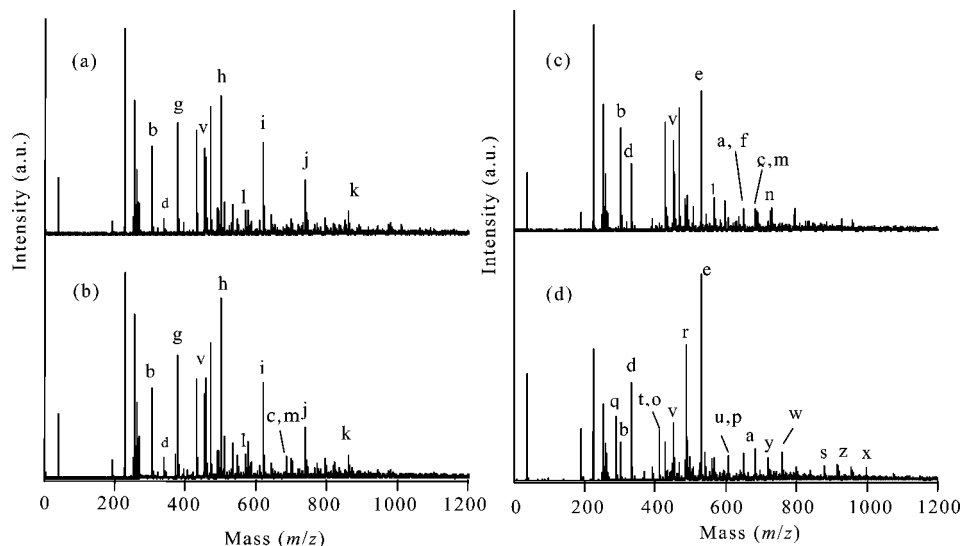


**Figure 10.** MALDI-TOF mass spectra of oligomers recovered after (a) 20 min, (b) 0.5 h, (c) 1 h, and (d) 6 h.

**Table 2. Structural Assignments of Peaks in Figure 10**

Peak code <sup>a</sup>	Mass (m/z)					Assignment <sup>b</sup>	
	Obs.				Calc.	m n	Structure
	20 min	0.5 h	1 h	6 h			
a	-	-	650.05	649.78	649.67	0 3	$\text{H}^+ \text{H}_3\text{CC}(\text{OB})_m \text{co}(\text{OPB})_n \text{OH}$
b	302.66	302.64	302.79	302.68	301.27	2 0	
c	-	688.25	688.21	-	687.77	0 3	$\text{K}^+ \text{H}_3\text{CC}(\text{OPB})_n \text{OH}$
d	332.86	332.94	332.90	332.75	333.45	0 1	
e	529.55	729.60	529.65	529.40	529.65	0 2	
f	-	-	650.05	-	649.76	1 2	$\text{K}^+ \text{H}_3\text{CC}(\text{OB})_m \text{co}(\text{OPB})_n \text{OK}$
g	376.91	376.89	-	-	377.46	2 0	
h	497.29	497.28	-	-	497.57	3 0	
i	617.65	617.63	-	-	617.67	4 0	
j	737.92	737.98	-	-	737.78	5 0	
k	858.23	858.29	-	-	857.89	6 0	
l	567.74	567.77	567.73	-	567.75	0 2	$\text{K}^+ \text{H}_2\text{KC}(\text{OB})_m \text{co}(\text{OPB})_n \text{OK}$
m	-	688.25	688.21	-	687.85	1 2	
n	-	-	703.34	-	729.80	0 3	$\text{K}^+ \text{H}_3\text{C}(\text{OPB})_n \text{OCCCH}_3$
o	-	-	-	411.03	411.43	0 2	$\text{H}^+ \text{H}(\text{OPB})_n \text{OH}$
p	-	-	-	607.64	607.64	0 3	
q	-	-	-	290.60	291.41	0 1	
r	-	-	-	487.27	487.62	0 2	$\text{K}^+ \text{H}(\text{OB})_m \text{co}(\text{OPB})_n \text{OK}$
s	-	-	-	878.50	880.03	0 4	
t	-	-	-	411.03	411.52	1 1	
u	-	-	-	607.64	607.72	1 2	
v	429.30	429.28	429.49	429.27	429.50	0 1	$\text{K}^+ (\text{OPB})_n \text{O}-\text{C}_6\text{H}_4-\text{C}_6\text{H}_4-\text{C}^+$
w	-	-	-	758.17	758.73	5 0	$\text{K}^+ (\text{OB})_m \text{co}(\text{OPB})_n \text{O}-\text{C}_6\text{H}_4-\text{C}^+$
x	-	-	-	954.69	954.94	5 1	
y	-	-	-	720.06	720.62	6 0	$(\text{OB})_m \text{co}(\text{OPB})_n$
z	-	-	-	916.60	916.85	6 1	

<sup>a</sup> Peak codes were shown in Figure 10. <sup>b</sup> OB: 4-oxybenzoyl unit. OPB: 4-(oxyphenyl)benzoyl unit.

of the needlelike crystals; thus the polymer molecules were aligned along the long axis of the needlelike crystals. In contrast to this, the diffraction pattern of the spindlelike crystals prepared for 1 h was totally different from that obtained from the tip of the needlelike crystals; it is attributable to a POB crystal as

assigned in Figure 8b. Reflections from a POBP crystal were not observed. {006} and {020} reflections of a POB crystal were detected on the meridian and the equator, respectively. The spindlelike crystals were comprised of POB. The spindlelike crystal prepared for 1 h was also observed by TEM after

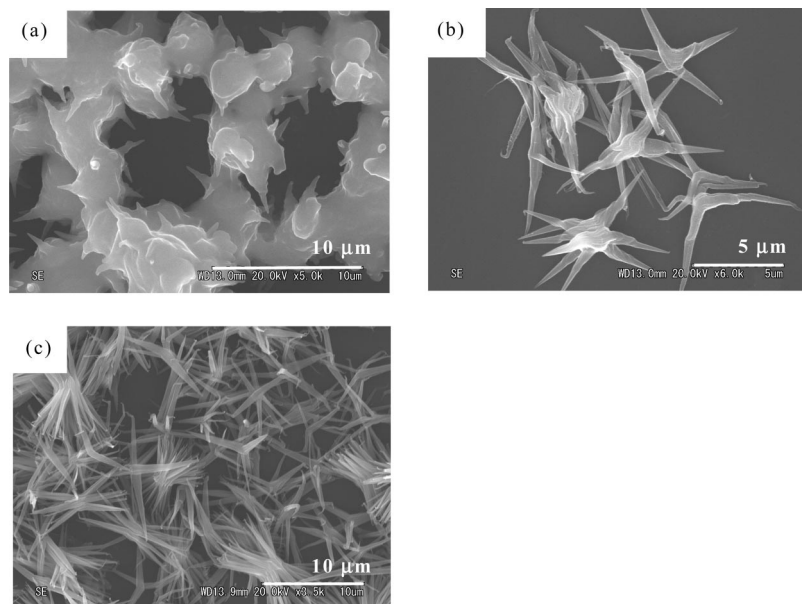


**Figure 11.** Morphologies of precipitates prepared from ABAD and APBA for  $\chi_f$  of (a) 25 mol % (run no. 10), (b) 20 mol % (run no. 11), and (c) 10 mol % (run no. 12).

shadowing with platinum–palladium to evaluate the thickness as shown in Figure 9. This crystal is  $3.0\ \mu\text{m}$  in thickness,  $4.6\ \mu\text{m}$  in width and  $5.3\ \mu\text{m}$  in length, and this is not a lamella. The  $\{020\}$  reflection of a POB crystal was also detected on the equator. The polymer molecules were aligned along the long axis of the spindlelike crystals. These results clearly indicate the formation feature of the needlelike crystals. As shown in Figure 5 (b), the spindlelike crystals were initially formed by the crystallization of the oligomers rich in OB moiety and then they grew to the needlelike crystals by the crystallization of the oligomers rich in OPB moiety on the spindlelike crystals.

Oligomers were recovered from the solution after 20 min, 0.5 h, 1 h, and 6 h, and analyzed by MALDI–TOF mass spectrometry. The spectra are shown in Figure 10 and the peak assignments are presented in Table 2. Many kinds of linear and cyclic oligomers consisting of 6 or 7 monomer moieties were detected from 20 min to 6 h, and the low molecular weight oligomers were precipitated to form the crystals throughout the polymerization. From the standpoint of the composition, the homo-oligomers of OB and OPB moiety were observed up to 0.5 h with co-oligomers. After 1 h, the oligomers rich in OB moiety decreased with time. The oligomers rich in OPB moiety were detected throughout the polymerization. This result reveals that the oligomers rich in OB moiety were phase-separated intensively at an initial stage of polymerization from 0.5 to 1 h with those rich in OPB moiety. The oligomers rich in OPB moiety were formed and phase-separated even after a middle stage. Although this discussion is based on the qualitative analysis, it is consistent with the above discussion.

From these results, the formation mechanism of the two different types of crystals is as follows; Homo-oligomers and co-oligomers are formed in the solution. When the molecular weight of oligomers exceeds the critical value, they are phase-separated through the supersaturated state. Among the oligomers, the OPB homo-oligomers and the co-oligomers rich in OPB moiety are rapidly precipitated due to the lower solubility, and they form the slablike crystals. Then OB homo-oligomers and the co-oligomers rich in OB moiety are precipitated via crystallization. They are segregated from the POBP slablike crystals and form the spindlelike POB crystals. The OPB homo-oligomers and the co-oligomers rich in OPB moiety are continuously precipitated and the slablike crystals grow. Usually,

the OPB homo-oligomers and the co-oligomers rich in OPB moiety are excluded from the POB crystals. However, the degree of supersaturation of oligomers is quite high during the initial stage of polymerization and, therefore, the OPB homo-oligomers and the co-oligomers rich in OPB moiety are added into the spindlelike POB crystals by the polymerization at the crystallization steps, leading to the formation of needlelike POBP crystals. Polymerization occurred on and in the crystals between oligomers. Finally needlelike and slablike crystals are simultaneously and separately formed with the aid of copolymerization.

**Polymerization of ABAD and APBA.** On the basis of the formation mechanism of needlelike POBP crystals in the copolymerization of ABA and APBA, if the oligomers rich in OB moiety can be more selectively precipitated during the initial stage of the polymerization, it is of great advantage to prepare the needlelike POBP crystals. ABAD, which is a dimer of ABA, was used for the copolymerization with ABPA instead of ABA. Polymerizations were carried out in DBT at a concentration of 1.0% at  $330\ ^\circ\text{C}$ . The results are also presented in Table 1 and the morphologies of the precipitates are shown in Figure 11. Although spherical precipitates were obtained at  $\chi_f$  of 25 mol %, needlelike crystals were formed at  $\chi_f$  of 20 and 10 mol %. The average length and width of the needlelike crystals prepared at  $\chi_f$  of 10 mol % were  $17.0$  and  $1.5\ \mu\text{m}$ , respectively. The value of  $\chi_p$  was 8 mol %. The fibrillated slablike crystals formed in the copolymerization of ABA and APBA were hardly observed in the copolymerization of ABAD and APBA at  $\chi_f$  of 10 mol %. In WAXS intensity profiles of the precipitates prepared at  $\chi_f$  of 10 mol %, the diffraction peaks were clearly observed at  $2\theta$  of  $19.3$ ,  $20.0$ ,  $23.5$ ,  $28.9$ ,  $29.8$ ,  $39.0^\circ$  as shown in Figure 3e and this profile is similar to that prepared from the copolymerization of ABA and APBA at  $\chi_f$  of 10 mol %, as shown in Figure 3d. The needlelike crystals possess quite high crystallinity.

## Conclusions

The copolymerization of ABA and APBA changed drastically the morphology of the crystals. At  $\chi_f$  of 90 to 25 mol %, the clear crystal habit was extinguished and spherical precipitates were obtained via liquid–liquid phase separation of the oligo-



mers. When the  $\chi_f$  was 20 and 10 mol %, starlike aggregates of needlelike crystals and fibrillated slablike crystals were separately formed, exhibiting similar morphology to POB and POBP homopolymer crystals. The homo-oligomers of OPB and the co-oligomers rich in OPB were more rapidly precipitated due to their lower solubility, and the slablike crystals were formed. The OB homo-oligomers and the co-oligomers rich in OB were precipitated to form the spindlelike crystals. The homo-oligomers of OPB and the co-oligomers rich in OPB were continuously precipitated, and the slablike crystals and the spindlelike crystals grew by their crystallization. Solid-state polymerization occurred between the oligomers in the precipitated crystals. Two kinds of crystals having different morphology and composition could be fabricated by means of the incorporation of the crystallization process in the copolymerization, and this result provides a new morphology control method for copolymerization systems.

## References and Notes

- (1) for examples: Seymour, R. B.; Krishenbaum, G. S. *High Performance Polymers: Their Origin and Development*; Elsevier Science Publishing: New York 1986.
- (2) Economy, J.; Storm, R. S.; Matkovich, V. I.; Cottis, S. G.; Nowak, B. E. *J. Polym. Sci., Polym. Chem. Ed.* **1976**, *14*, 2207.
- (3) Economy, J.; Storm, R. S. *Macromol. Monogr.* **1977**, *3*, 45.
- (4) Economy, J.; Volksen, W.; Geiss, R. H. *Mol. Cryst. Liq. Cryst.* **1984**, *105*, 289.
- (5) Lieser, G.; Schwarz, G.; Kricheldorf, H. R. *J. Polym. Sci., Polym. Phys. Ed.* **1983**, *2*, 1–1599.
- (6) Schwarz, G.; Kricheldorf, H. R. *Makromol. Chem. Rapid Commun.* **1988**, *9*, 717.
- (7) Kimura, K.; Kohama, S.; Yamazaki, S. *Polym. J.* **2006**, *38*, 1005.
- (8) Yamashita, T.; Kato, Y.; Endo, S.; Kimura, K. *Makromol. Chem. Rapid Commun.* **1988**, *9*, 687.
- (9) Yamashita, Y.; Kimura, K. *Polymeric Materials Encyclopedia*; CRC Press: Boca Raton, FL, 1996, 8707.
- (10) Kricheldorf, H. R.; Ruhser, F.; Schwarz, G.; Adebahr, T. *Makromol. Chem.* **1991**, *192*, 2371.
- (11) Kricheldorf, H. R.; Schwarz, G.; Ruhser, F. *Macromolecules* **1991**, *24*, 3485.
- (12) Kimura, K.; Kato, Y.; Inaba, T.; Yamashita, Y. *Macromolecules* **1995**, *28*, 255.
- (13) Schwarz, G.; Kricheldorf, H. R. *Macromolecules* **1995**, *28*, 3911.
- (14) Liu, J.; Rybnikar, F.; East, A. J.; Geil, P. H. *J. Polym. Sci., Part B: Polym. Phys.* **1993**, *31*, 1923.
- (15) Rybnikar, F.; Yuan, B.-L.; Geil, P. H. *Polymer* **1994**, *35*, 1831.
- (16) Liu, J.; Rybnikar, F.; Geil, P. H. *J. Macromol. Sci., Phys.* **1996**, *B35*, 375.
- (17) Lucero, A.; Rybnikar, F.; Long, T.-C.; Liu, J.; Geil, P. H.; Wall, B.; Koenig, J. L. *Polymer* **1997**, *38*, 4387.
- (18) Kimura, K.; Nakajima, D.; Kobashi, K.; Yamashita, Y.; Yokoyama, F.; Uchida, T.; Sakaguchi, Y. *Polym. Adv. Tech.* **2000**, *11*, 747.
- (19) Schwarz, G.; Zemmann, U.; Kricheldorf, H. R. *High Perform. Polym.* **1997**, *9*, 61.
- (20) Kricheldorf, H. R.; Adebahr, T. *J. Polym. Sci., Part A: Polym. Chem.* **1994**, *32*, 159.
- (21) Kricheldorf, H. R.; Loehden, G.; Wilson, D. J. *Macromolecules* **1994**, *27*, 1669.
- (22) Kimura, K.; Kobashi, K.; Maeda, H.; Yamashita, Y. *Macromol. Rapid Commun.* **2003**, *24*, 190.
- (23) Kricheldorf, H. R.; Adebahr, T. *J. Polym. Sci., Part A: Polym. Chem.* **1994**, *32*, 159.
- (24) Schwarz, G.; Zemmann, U.; Kricheldorf, H. R. *High Perform. Polym.* **1997**, *9*, 61.
- (25) Kobashi, K.; Kimura, K.; Yamashita, Y. *Macromolecules* **2004**, *37*, 7570.
- (26) Somogyi, A.; Bojkova, N.; Padias, B. A.; Hall, H. K., Jr. *Macromolecules* **2005**, *38*, 4067.
- (27) Scamporrino, E.; Vitalini, D.; Mineo, P. *Macromolecules* **1996**, *29*, 5520.
- (28) Gies, A. P.; Hercules, D. M.; Ellison, S. T.; Nonidez, W. K. *Macromolecules* **2006**, *39*, 941.
- (29) J.Liu, J.; Yuan, B.-L.; Geil, P. H.; Dorset, D. L. *Polymer* **1997**, *38*, 6031.

MA800029N